Metathetical Synthesis of Binary and Ternary Antiferromagnetic Gadolinium Pnictides (P, As, and Sb)

Randolph E. Treece,† Jeanine A. Conklin,† and Richard B. Kaner*

Department of Chemistry and Biochemistry and Solid State Science Center, University of California, Los Angeles, California 90024-1569

Received May 10, 1994[⊗]

Polycrystalline powders of new ternary phases and well-known binary "III−V" type antiferromagnetic gadolinium pnictides have been prepared in seconds by rapid solid-state metathesis (exchange) reactions: $GdI_3 + Na_3Pn \rightarrow GdPn + 3NaI$ (where Pn = pnictogen = P, As, Sb, or P_xAs_{1-x}). Following thorough mixing of the precursors, the reactions are initiated by local heating with a hot filament and the products are easily isolated by washing with methanol and water. The effectiveness of the solid-state metathesis (SSM) process is shown by comparing the precursor reaction products to those generated by the direct combination of the elements at elevated temperatures (1000 °C for 100 h). Characterization techniques include powder X-ray diffraction (XRD), magnetic susceptibility, scanning electron microscopy, and energy dispersive X-ray analysis (EDX). The rapidly generated SSM products are single-phase, antiferromagnetic, XRD- and EDX-pure powders, comparable to the compounds prepared by heating the elements together for several days. Slight traces of ferromagnetic gadolinium, as revealed by field-dependent magnetization, are removed and the average particle size is increased by a 12 h anneal at 1000 °C. The new gadolinium phosphide−arsenide solid solutions display magnetic constants (T_N and Θ_p) intermediate between those of their binary progenitors.

Rare-earth pnictide "III−V" type compounds, made up of a group 3 metal (Y, La, Ce, ..., Lu) and a group 15 nonmetal (N, P, As, and Sb = pnictogen = Pn) in one to one stoichiometry, have been compared to the traditional III−V compounds (group 13−15 by IUPAC convention), such as GaAs. The group 13−15 compounds are well-known semiconductors, and early theoretical considerations led to the postulation that the rare-earth phosphides, nitrides, and some arsenides might be semiconductors with energy gaps as great as 2.5 eV.[1] Predictions of semiconducting behavior, coupled with ferromagnetic or antiferromagnetic properties displayed by these materials, led to extensive investigations into the intrinsic properties of these "magnetic semiconductors". The intrinsic electronic properties of the rare earth pnictides (REPn's), as either semiconductors, semimetals, or metals, is still the subject of speculation,[2−6] and deviation from ideal one to one stoichiometry has been suggested as a cause for conflicting experimental determinations.[5] Preparation of stoichiometric samples is confounded by the reactive nature of the lanthanide metals, the differing vapor pressures of the starting materials, and the very high melting points of the one to one compounds (>2200 °C). Early synthetic approaches to REPn's resemble traditional solid-state chemistry techniques, where the preparation of REPn powders has been accomplished by several high-temperature elemental and precursor methods. The REPn's have been prepared by direct solid-solid reactions in sealed ampules,[2,7] under pressure[8] and by solid−gas processes.[9] Both single-source and gas-phase precursors have also been used to make the REPn's.[10,11]

Solid-state precursor reactions can overcome the long times and high temperatures associated with traditional synthetic methods. In addition, many of the hazards of working with toxic phosphine and arsine in the gas-phase precursor reactions are avoided. Solid-state precursors have already been used to prepare polycrystalline refractory materials,[12] binary and ternary transition-metal dichalcogenides and oxides,[13] lanthanide chalcogenides and pnictides,[14] and binary and ternary III−V compound semiconductors.[12,14ac,15] Here we describe the prepa-

† Current address: Naval Research Laboratory, Surface Modification Branch (Code 6670), Washington, DC 20375-5345.

[⊗] Abstract published in *Advance ACS Abstracts,* November 1, 1994.

(1) Sclar, N. *J. Appl. Phys.* **1962**, *33*, 2999.
(2) Hiscocks, S. E. R. and Mullin, J. B. *J. Mater. Sci.* **1969**, *4*, 1969.
(3) Busch, G. *J. Appl. Phys.* **1967**, *38*, 1967.
(4) Wachter, P. *CRC Crit. Rev. Solid State Sci.* **1972**, *3/I2*, 189.
(5) Hulliger, F. in *Handbook on the Chemistry and Physics of Rare Earths;* Gschneidner, K. A., Eyring, L., Eds.; North-Holland Publishing Co.: New York, 1979, Vol. 4, p 153.
(6) Some rare-earth arsenides have been epitaxially grown on semiconductors, as described in (a) Palmstrøm, C. J.; Tabatabaie, N.; Allen, S. J., Jr. *Appl. Phys. Lett.*, **1988**, *53*, 2608. (b) Allen, S. J.; Tabatabaie, N.; Palmstrøm, C. J.; Hull, G. W.; Sands, T.; DeRosa, F.; Gilchrist, H. L.; Garrison, K. C. *Phys. Rev. Lett.*, **1989**, *62*, 2309. (c) Palmstrøm, C. J.; Garrison, K. C.; Mounier, S.; Sands, C. L.; Schwartz, C. L.; Tabatabaie, N.; Allen, S. J.; Gilchrist, H. L.; Miceli, P. F. *J. Vac. Sci. Technol. B.*, **1989**, *7*, 747. (d) The possibility that YbAs might be a heavy fermion system is described in Monnier, R.; Degiorgy, L.; Delly, B.; and Koelling, D. D. *Physica B* **1990**, *163*, 110.
(7) Iandelli, A. In *Rare Earth Research*, Kleber, E. V., Ed.; Macmillan Co.: New York, 1961; p 135.
(8) LaValle, D. E. *J. Inorg. Nucl. Chem.* **1962**, *24*, 935.
(9) Miller, J. F.; Himes, R. C. in *Rare Earth Research*, Kleber, E. V., Ed.; Macmillan Co.: New York, 1961; p 232.
(10) Howell, J. K.; Pytlewski, L. L. *Inorg. Nucl. Chem. Lett.* **1970**, *6*, 681.
(11) Yim, W. M.; Stofko, E. J.; Smith, R. T. *J. Appl. Phys.* **1972**, *43*, 254.
(12) (a) Wiley, J. B.; Kaner, R. B. *Science* **1992**, *255*, 1093−1097. (b) Treece, R. E; Gillan, E. G.; Jacubinas, R. M.; Wiley, J. B.; Kaner, R. B. *Better Ceramics Through Chemistry V*; Hampden-Smith, M. J., Klemperer, W. J., Brinker, C. J., Eds.; MRS Symp. Proc. Vol. 271; Materials Research Society: Pittsburgh, PA, 1992; pp 169−174. (c) Kaner, R.; Bonneau, P.; Gillan, E.; Wiley, J.; Jarvis, R., Jr.; Treece, R., U.S. Pat. No. 5,110,768, 1992. (d) Ponthieu, E.; Rao, L.; Gengembre, L.; Grimblot, J.; Kaner, R. B. *Solid State Ionics* **1992**, *63*−65, 116.
(13) (a) Bonneau, P. R.; Shibao, R. K.; and Kaner, R. B. *Inorg. Chem.* **1990**,*29*, 2511(b) Bonneau, P. R.; Jarvis, R. F., Jr.; Kaner, R. B *Nature* **1991**,*349*, 510. (c) Bonneau, P. R.; Jarvis, R. F., Jr.; Kaner, R. B. *Inorg. Chem.* **1992**, *31*, 2127. (d) Wiley, J.; Bonneau, P.; Treece, R.; Jarvis, R., Jr.; Gillan, E.; Rao, L.; Kaner, R In *Supramolecular Architecture : Synthetic Control in Thin Films and Solids,* Bein, T., Ed.; ACS Symposium Series 499; American Chemical Society: Washington, DC, 1992; pp 367−383. (e) Bonneau, P. R.; Wiley, J. B.; Kaner, R. B. *Inorg. Synth.*, in press. (f) Wiley, J. B.; Gillan, E. G.; Kaner, R. B. *Mater. Res. Bull.* **1993**, *28*, 893.

0020-1669/94/1333-5701$04.50/0

ration and characterization of binary and ternary antiferromagnetic gadolinium pnictides by rapid, self-sustaining precursor reactions. The effectiveness of the ignited solid-state metathesis (SSM) process is shown by comparing the precursor reaction products to those generated by the direct combination of the elements at elevated temperatures (1000 °C for 100 h), using the characterization techniques of powder X-ray diffraction (XRD), magnetic susceptibility, scanning electron microscopy, and energy dispersive X-ray analysis (EDX).

Experimental Section

Gadolinium iodide (GdI_3) was made from the elements at *ca.* 800 °C in sealed silica ampules, and then purified by direct vapor transport in a 900 °C−room temperature gradient. The sodium pnictides were prepared by heating stoichiometric amounts of the constituent elements in sealed Pyrex ampules at 550 °C for 5 h, opening the tubes and grinding the contents in a He-filled drybox, reloading and sealing the contents under vacuum, and reheating for an additional five hours at 500 °C. Ternary solid-solution pnictide precursors, $Na_3(P,As)$ having nominal phosphorus:arsenic ratios of 75:25, 50:50, and 25:75 were also prepared. The homogeneity and composition of the solid-solution precursors were verified by powder XRD. The materials are single phase, and the hexagonal cell volumes correspond to compositions of $Na_3P_{0.77(2)}As_{0.23(2)}$, $Na_3P_{0.52(2)}As_{0.48(2)}$, and $Na_3P_{0.28(2)}As_{0.72(2)}$, assuming a linear relationship between the composition and volume of the solid solutions. (*Caution*! The sodium pnictides are toxic and highly reactive to air and water.)

Ignition Precursor Reactions. The gadolinium pnictides were prepared by igniting the solid-state precursor reaction

$$GdI_3 + Na_3Pn \xrightarrow{\text{ignite}} \text{i-GdPn} + 3NaI \qquad (1)$$

where Pn = P, As, Sb, or P_xAs_{1-x} (i = ignited). The gadolinium (III) iodide and sodium pnictide precursors were ground separately with a mortar and pestle in a He-filled drybox, mixed in equimolar quantities, and then ignited with a hot filament in a bomb similar to those used in calorimetry experiments.[13e] The products were ground in a drybox and then washed in air with methanol, water and diethyl ether to remove the sodium iodide byproduct and any unreacted starting reagents. The isolated products were dried on a vacuum line for 8 h.

Annealed Ignition Reactions. Portions of the ignited products generated by eq 1 were also annealed by heating in clean, dry ampules. These products were ground with a mortar and pestle in a He-filled drybox and then loaded into silica tubes which were sealed under vacuum and heated to 1000 °C for 12 h, according to eq 2. The annealed materials were isolated as described above (a = annealed).

$$GdPn + 3NaI \xrightarrow[\text{(2) wash}]{\text{(1) 1000 °C/12 h}} \text{a-GdPn} \qquad (2)$$

Direct Elemental Reactions. Gadolinium pnictides were also prepared from the elements according to eq 3, where Pn = P, As, Sb,

$$Gd + Pn\ (\text{powder}) \xrightarrow[\text{(2) pulverize}]{\text{(1) 1000 °C/50 h}} \xrightarrow{\text{(3) 1000 °C/50 h}} \text{ht-GdPn} \qquad (3)$$

or stoichiometric ratios of P and As (ht = high temperature). Gadolinium powder (Cerac 99.9%, −40 mesh) and either red phosphorus powder (Alfa, −100 mesh), arsenic powder (Aldrich, 99.999+), antimony powder (Aldrich, 99.999+), or a mixture of phosphorus and arsenic were mixed together and sealed in evacuated (10^{-5} Torr) silica ampules. The ampules were slowly heated to 1000 °C over 4 h and allowed to anneal for 12 h.[2] The tubes were then cooled, the contents removed, ground in a He-filled drybox, resealed under vacuum, and reheated at 1000 °C for 50 h. This grinding and reheating was repeated twice for a total heating period of greater than 100 h.

Characterization. Powder XRD patterns of the precursors and the products were obtained on a $\theta-2\theta$ Crystal Logic powder diffractometer with graphite monochromated Cu K_α radiation, scanning in steps of 0.02° 2Θ at a rate of 10 s/step. Using the XLAB program,[16a] the XRD data was fit, the Cu $K_{\alpha 2}$ lines subtracted out, and the lattice parameter determined by least squares refinement. Average particle size was determined by the method of Scherrer and Warren, relative to an internal tungsten standard.[16b] The magnetic susceptibility measurements were performed on a SHE Corporation 905 SQUID, in the temperature range from 5 to 360 K, on samples varying in size from 20 to 70 mg. Values for the paramagnetic Curie temperatures, Θ_p, and the effective magnetic moments, μ_{eff}, were determined from linear extrapolation of the inverse susceptibility versus temperature data between 50−360 K using the Curie−Weiss law. The Néel temperatures, T_N, were taken from the minimum in the inverse susceptibility versus temperature plots. The exchange constants J_1 and J_2 were calculated using the molecular-field approximation from the experimental values of T_N and Θ_p, assuming only nearest-neighbor (nn) and next-nearest-neighbor (nnn) interactions, by

$$T_N = (-)\,4J_2S(S+1) \qquad (4)$$

and

$$\Theta_p = 4S(S+1)(6J_1 + J_2) \qquad (5)$$

where $S = {}^7/_2$ for Gd^{3+}, and J_1 and J_2 are in temperature units of K.[17]

The amount of free gadolinium metal within the GdPn products was determined by the method of Honda and Owens, where the susceptibility is measured as a function of the applied magnetic field.[18] The Honda−Owens (H-O) measurements were performed at 280 K (T_C for Gd = 293 K), corresponding to the maximum deviation from Curie−Weiss behavior in $1/\chi$ vs T plots. Analysis was performed on susceptibility versus inverse field data using $\chi_t = \chi_p + \sigma/H$, where χ_t is the measured total susceptibility of the sample, χ_p is the intrinsic paramagnetic susceptibility of the sample, σ is the magnetization of the ferromagnetic impurity (Gd metal in this case), and H is the applied field. Fields of 2, 5, 10, 20, and 40 kOe were used in these experiments.

The scanning electron microscopy (SEM) was performed on a Cambridge SEM with a LaB_6 tip. Using a Link AN10000 energy dispersive analyzer attached to the SEM, qualitative elemental analyses were performed by energy dispersive X-ray analysis (EDX). Regional homogeneity within the products was confirmed by performing EDX on various regions across the sample surface, using both area scans (at different magnifications) and point scans.

Results

Binary and mixed-anion ternary GdPn materials have been prepared both by SSM methods with reactive precursors and by heating the appropriate rare-earth metal and pnictogen elements in sealed tubes. The SSM approach includes both the ignited precursor reactions and the annealed ignition products. The materials were characterized by powder XRD, EDX, and magnetic susceptibility. This paper will compare similar compounds made by the different methods and examine possible reaction pathways for the rapid SSM processes.

Structural and Compositional Characterization. The reactants, reaction conditions and products of the three synthetic

(14) (a) Treece, R. E., Ph.D. Thesis, University of California, Los Angeles, 1992. (b) Rowley, A. T.; Parkin, I. P. *J. Mater. Chem.* **1993**, *3*, 689. (c) Treece, R. E.; Kaner, R. B. *Ceram. Ind. Int.* **1993**, *103*, 8. (d) Fitzmaurice, J. C.; Parkin, I. P.; Rowley, A. T. *J. Mater. Chem.* **1994**, *4*, 285. (e) Hector, A. L.; Parkin, I. P. *Z. Naturforsch.* **1994**, *496*, 477.

(15) (a) Treece, R. E.; Macala, G. S.; Kaner, R. B. *Chem. Mater.* **1992**, *4*, 9. (b) Treece, R. E.; Macala, G. S.; Franke, D.; Rao, L.; Eckert, H.; Kaner, R. B. *Inorg. Chem.* **1993**, *32*, 2745. (c) Franke, D.; Treece, R. E.; Kaner, R. B; Eckert, H. *Anal. Chem. Acta* **1993**, *283*, 987. (d) Treece, R. E.; Gillan, E. G.; Kaner, R. B. *Comments Inorg. Chem.* **1994**, *16*, 313. (e) Treece, R. E.; Bonneau, P. R.; Kaner, R. B. *Mater. Res. Bull.*, submitted for publication.

(16) (a) W. Dollace, Department of Geology, University of California, Los Angeles, CA 90024. (b) Cullity, B. O. *Elements of X-ray Diffraction*; Macmillan, New York, 1990.

(17) Jones, E. D. and Morosin, B. *Phys. Rev.* **1967**, *160*, 451.

(18) Honda, K. *Ann. Phys.* **1912**, *37*, 657. (b) Honda, K. *Magnetic Properties of Matter*, Syokwabo and Company: Tokyo, Japan, 1928.

Table 1. Summary of Reactions and XRD Results[a]

reactants	method	product[b]	a_o (Å)	reported a_o (Å)	av particle size (Å)
$GdI_3 + Na_3P$	ignite	i-GdP	5.732(1)	5.723[7] and 5.74[20]	750
	ignite + anneal	a-GdP	5.728(1)		>2000
Gd + P (red)	1000 °C/100 h	ht-GdP	5.728(1)		>2000
$GdI_3 + Na_3P_{0.77(2)}As_{0.23(2)}$	ignite + anneal	$a\text{-}GdP_{0.72(2)}As_{0.28(2)}$	5.765(1)		1970
$Gd + {}^3/_4P$ (red) + ${}^1/_4As$	1000 °C/100 h	$ht\text{-}GdP_{0.76(2)}As_{0.24(2)}$	5.759(1)		>2000
$GdI_3 + Na_3P_{0.52(2)}As_{0.48(2)}$	ignite	$i\text{-}GdP_{0.51(2)}As_{0.49(2)}$	5.792(1)		450
	ignite + anneal	$a\text{-}GdP_{0.49(2)}As_{0.51(2)}$	5.795(1)		1970
$Gd + {}^1/_2$(red) + ${}^1/_2As$	1000 °C/100 h	$ht\text{-}GdP_{0.51(2)}As_{0.49(2)}$	5.792(1)		1500
$GdI_3 + Na_3P_{0.28(2)}As_{0.72(2)}$	ignite + anneal	$a\text{-}GdP_{0.23(2)}As_{0.77(2)}$	5.830(5)		1180
$Gd + {}^1/_4P$(red) + ${}^3/_4As$	1000 °C/100 h	$ht\text{-}GdP_{0.30(2)}As_{0.70(2)}$	5.820(1)		1100
$GdI_3 + Na_3As$	ignite	i-GdAs	5.860(1)	5.854[21] and 5.866[17]	650
	ignite + anneal	a-GdAs	5.860(1)		1800
Gd + As	1000 °C/100 h	ht-GdAs	5.863(1)		1120
$GdI_3 + Na_3Sb$	ignite	i-GdSb	6.24(1)		580
	ignite + anneal	a-GdSb	6.219(1)	6.217(7)	980
Gd + Sb	1000 °C/100 h	ht-GdSb	6.217(1)		1100

[a] Key: i = ignited; a = annealed; ht = high temperature. [b] NaI was a crystalline product in every reaction.

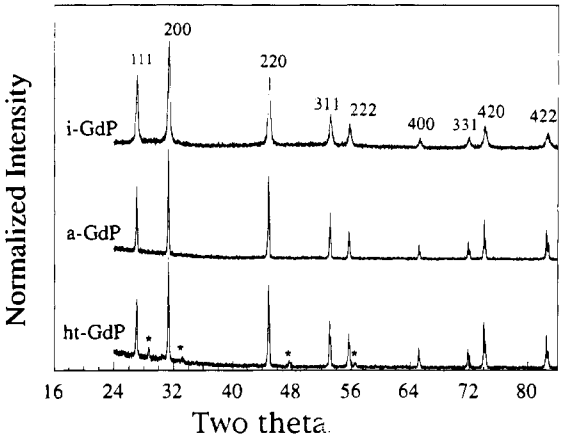

Figure 1. Powder XRD patterns of the GdP ignition products before (i-GdP) and after (a-GdP) annealing, and the materials made from the elements (ht-GdP). The Miller indices are indicated on the top trace, and the asterisks identify peaks arising from Gd_2O_3 impurities.

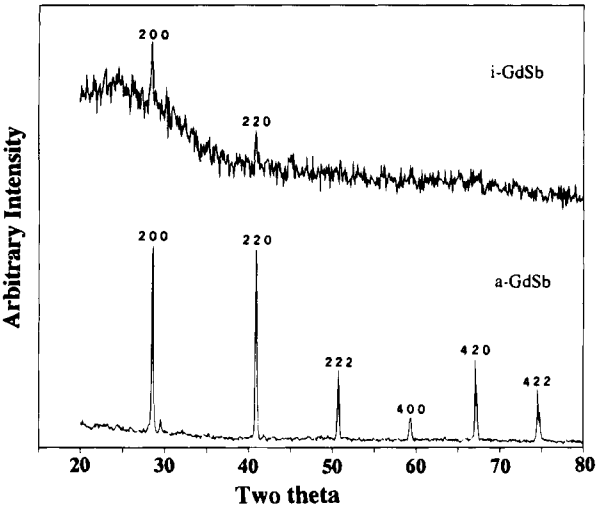

Figure 2. Powder XRD patterns of GdSb ignition products before (i-GdSb) and after (a-GdSb) annealing.

methods are summarized in Table 1. In general, the washed products were found by SEM to be fine-grained, homogeneous powders, and there was no sodium or iodine detectable by EDX analyses. Also presented in Table 1, in addition to the reaction information, are the results of powder XRD studies, including measured and previously reported a_o values and average particle sizes. The series of GdP compounds will be discussed in detail as it is representative of the other Gd pnictides. Figure 1 shows XRD patterns of single-phase GdP prepared by the three methods described above with all of the characteristic XRD peaks for the rock salt structure.[7] While the three GdP compounds have essentially identical lattice parameters, broadening of the XRD peaks due to particle size effects is apparent in the trace of i-GdP. After annealing the ignition compound, the diffraction lines for a-GdP narrowed, indicating particle growth. The crytallinities of a-GdP and ht-GdP (the material made from the elements at high temperature) are similar with particle sizes exceeding that measurable using XRD analysis (>2000 Å). A trace of Gd_2O_3 is present in the sample made from the elements.[19] This arises from surface oxidation of the metal powder and is present in the as-received gadolinium. Traces of Gd_2O_3 are detectable in most of the compounds prepared by the elemental route. The absence of these peaks in the products made by the two SSM methods is indicative of the high purity of the vapor-transported GdI_3 used in the precursor reactions.

The particle size of the i-GdPn materials decrease on going from P to Sb. The decreasing particle size is most apparent in the i-GdSb sample. In contrast to the i-GdP and i-GdAs materials prepared by the ignited SSM reactions, the i-GdSb samples were very poorly crystallized, with considerable amounts of both amorphous and polycrystalline GdSb (average particle size = 580 Å). The powder XRD pattern of the precursor ignition product (i-GdSb, Figure 2) revealed a very broad peak below 35° 2Θ with the *200* and *220* lines rising only slightly above the background noise. After annealing, the well known FCC structure became apparent in the XRD pattern (a-GdSb, Figure 2).

Solid solution materials of the compounds Gd(P, As) were prepared by the three methods described above. XRD patterns of the products made by the annealed ignition reactions are shown in Figure 3. To the best of our knowledge, these are the first mixed-anion solid solutions of the rare-earth pnictides to be characterized in bulk form. The compositions of the $a\text{-}GdP_xAs_{1-x}$ solid solutions were determined from their lattice

(19) The presence of traces of Gd_2O_3 in the GdPn materials have no detectable effect, within experimental error, since the oxides have paramagnetic properties similar to the pnictides (μ_{eff} = 7.8 μ_B and Θ_p = 17 K) and magnetically order at lower temperatures (T_N <4 K). (a) Arajs, S.; Colvin, R. V. *J. Appl. Phys.* **1962**, *33*, 2517. (b) Miller, A. E.; Jelinek, F. J.; Gschneidner, K. A., Jr.; Gerstein, B. C. *J. Chem. Phys.* **1971**, *55*, 2647.

(20) Kaldis, E.; von Schulthess, G.; Wachter, P. *Solid State Commun.* **1975**, *17*, 1401.

(21) Brixner, L. H. *J. Inorg. Nucl. Chem.* **1960**, *16*, 199.

Table 2. Summary of Magnetic Results for Binary Materials

sample	Θ_p (K)	reported Θ_p (K)	T_N (K)	reported T_N (K)	J_1 (K)	J_2 (K)	μ_{eff} (μ_B)	reported μ_{eff} (μ_B)
a-GdP	3(2)	(−2),[22] (0),[24] (+2),[3] and (+40)[7]	16.0(5)	13[7] and 15[22]	0.15(1)	−0.25(1)	7.9(2)	7.7[2,4] and 7.95[7]
ht-GdP	3(2)		16.0(5)		0.15(1)	−0.25(1)	7.9(2)	
a-GdAs	−10(2)	−12[24] and 6[7]	20.0(5)	25[25]	0.08(1)	−0.32(1)	7.8(2)	8.2[25]
ht-GdAs	−10(2)		20.0(5)		0.08(1)	−0.32(1)	7.8(2)	

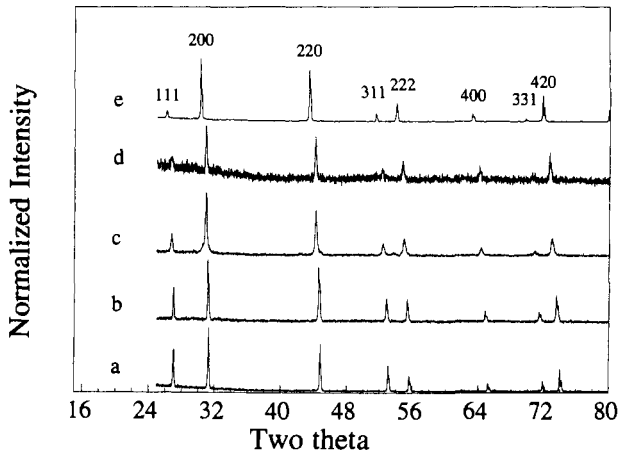

Figure 3. Powder XRD patterns for the a-Gd(P_xAs_{1-x}) samples with (a) $x = 1.0$, (b) $x = 0.72$, (c) $x = 0.49$, (d) $x = 0.23$, and (e) $x = 0.0$. The Miller indices are indicated on the top trace.

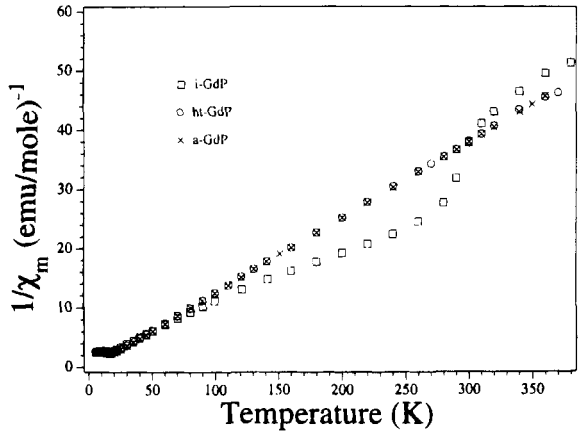

Figure 4. Plot of inverse molar susceptibility versus temperature for the three GdP samples. The presence of a ferromagnetic (Gd metal, T_C = 293 K) impurity is revealed by the dip in the i-GdP scan.

parameters assuming Vegard's Law, and the results are presented in Table 1. This is a reasonable assumption since the bonding in the GdPn materials have considerable ionic character, and it has been established that solid solutions of ionic materials, such as KCl−NaCl, are known to strictly follow Vegard's Law.[16b] It can be seen that the relative phosphorus and arsenic composition of the Gd(P, As) products are consistent with the solid-solution sodium pnictide precursors.

Magnetic Characterization. The magnetic susceptibility of the various samples was measured as a function of temperature at a field of 2 kOe, and the results for the binary materials are summarized in Table 2. Again, the results of the three GdP samples are representative and will be used for discussion. The magnetic data are plotted as inverse susceptibility versus temperature in Figure 4. All three samples ordered antiferromagnetically with T_N = 16.0(5) K, compared to reported values of 13 K[7] and 15 K.[22] At temperatures above T_N, the a-GdP and ht-GdP samples obey the Curie−Weiss law (the i-GdP samples are discussed below), and a linear fit of the inverse

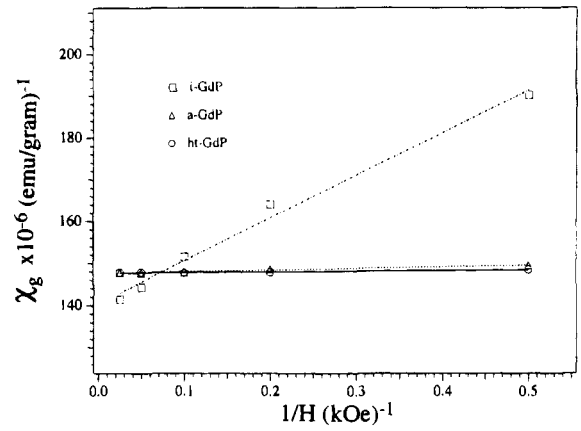

Figure 5. Honda−Owens plot of gram susceptibility versus inverse field for the three GdP samples. The amount of free gadolinium in the direct ignition product, determined from the slope of the i-GdP line, is 0.04% (10^{-5} g).

molar susceptibility versus temperature data between 50 and 360 K gives a paramagnetic Curie temperature of Θ_p = 3(2) K.[23] Values reported for Θ_p include (−2),[22] (0),[24] (+2)[3] and (+40)[7] K. The effective number of Bohr magnetons (μ_B) has also been determined for the materials from the high-temperature (T >50 K) paramagnetic data with μ_{eff} = 7.9(2) μ_B for both a-GdP and ht-GdP, which is between reported values of 7.7 μ_B[24] and 7.95 μ_B.[7] The theoretical value for the Gd^{3+} ion calculated from $\mu_{eff} = g\,[J\,(J+1)]^{1/2}$ is 7.94 μ_B.[3]

The i-GdP sample does not display Curie−Weiss behavior. The dip in the inverse susceptibility versus temperature plot arises from a ferromagnetic impurity within the sample, and all of the i-GdPn samples behaved similarly. The amount of ferromagnetic impurity was quantified by Honda−Owens (H-O) analysis (Figure 5). The H-O analysis was performed at 280 K, corresponding to the maximum difference in the inverse susceptibility versus temperature plot. The a-GdP and ht-GdP susceptibilities are independent of magnetic field, but the i-GdP sample shows increasing susceptibility with applied field strength. From the slope of the line the amount of free metal in i-GdP was determined to be 0.04% (10^{-5} g). In order to verify that the magnetic impurity was gadolinium, a H-O scan was performed on i-GdAs at 320 K, in addition to the run at 280 K (Figure 6). At 320 K, the measurement did not reveal any ferromagnetic impurity, since above its Curie temperature (293 K) gadolinium changes from a ferromagnetic to a paramagnetic state. The i-GdAs powder had a free metallic gadolinium content of 0.31%, and the amount in i-GdSb was determined to be 0.02%.

Ternary Materials. Plots of the inverse molar susceptibility versus temperature for the ht-Gd(P, As) series of products are shown in Figure 7. The inset in Figure 7 expands the low-temperature region, revealing that the Néel points of the three ternary materials are intermediate between the two binary

(22) Busch, G.; Junod, P.; Schwob, P.; Vogt, O.; Hulliger, F. *Phys. Lett.* **1964**, *9*, 7.

(23) Positive values for Θ_p typically mean that a material is ferromagnetic, but in the case of GdP, the intrinsic antiferromagnetic character of the compound has been unambiguously determined magnetically by various authors[7,17] and by low-temperature X-ray diffraction.[17]

(24) Busch, G.; Schwob, P.; Vogt, O.; Hulliger, F. *Phys. Lett.* **1964**, *11*, 100.

(25) Busch, G.; Vogt, O.; Hulliger, F. *Phys. Lett.* **1965**, *15*, 301.

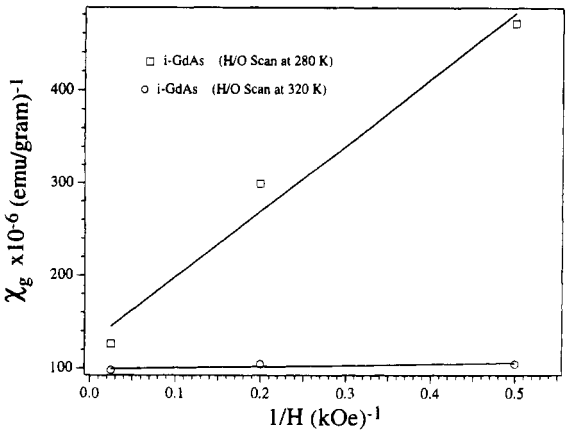

Figure 6. Honda–Owens plot of gram susceptibility versus inverse field for i-GdAs below (280 K) and above (320 K), the Curie temperature of gadolinium (T_C = 293 K).

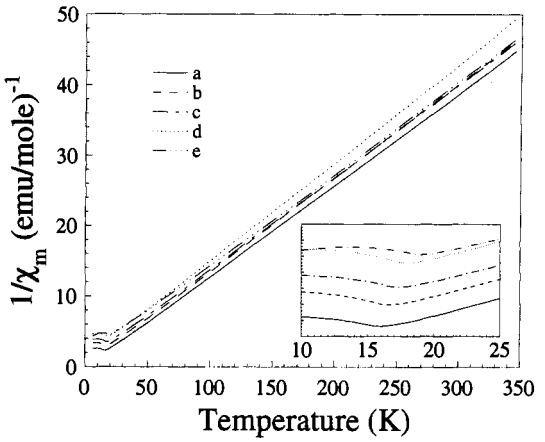

Figure 7. A plot of inverse molar susceptibility versus temperature for the ht-Gd(P_xAs_{1-x}) samples with (a) x = 1.0, (b) x = 0.76, (c) x = 0.51, (d) x = 0.30, and (e) x = 0.0. Inset shows an expanded view of the low temperature region.

compounds. The ternary compounds ht-$GdP_{0.76(2)}As_{0.24(2)}$, ht-$GdP_{0.51(2)}As_{0.49(2)}$, and ht-$GdP_{0.30(2)}As_{0.70(2)}$ order antiferromagnetically at T_N = 16.5(5) K, 17.5(5) K, and 18.0(5) K, respectively, and have respective paramagnetic Curie temperatures of Θ_p = −1(2) K, −4(2) K and −7(2) K. The amount of free metal in i-$GdP_{0.51}As_{0.49}$ was determined by H-O analysis to be 0.02%, and the μ_{eff} values for the ternary materials are consistent with those determined for the binary materials. The magnetic susceptibility results for the rest of the solid solution materials are presented in Table 3.

Values of T_N and Θ_p also have been modeled for various Gd(P,As) solid solutions. Assuming a linear relationship between the relative pnictide composition and the magnetic coupling constants, eqs 4 and 5 have been adapted to

$$\Theta_p = 4S(S+1)[6(X_{GdP}J_{1(GdP)} + X_{GdAs}J_{1(GdAs)}) + (X_{GdP}J_{2(GdP)} + X_{GdAs}J_{2(GdAs)})] \quad (6)$$

and

$$T_N = (-)\,4S(S+1)(X_{GdP}J_{2(GdP)} + X_{GdAs}J_{2(GdAs)}) \quad (7)$$

where $S = {}^7/_2$ for Gd^{3+}, and X_{GdPn} is the mole fraction of the binary pnictide based on the composition determined by XRD. The calculated T_N and Θ_p values for the ternary materials are presented in Table 3 with the experimental results. It can be seen that the measured and calculated values of T_N and Θ_p for each composition are the same within experimental errors. These calculations reveal that if one assumes a linear relationship between composition and susceptibility for the ternary Gd(P, As) compounds, the stoichiometries determined by XRD are consistent with those found by magnetic susceptibility, within experimental errors.

Table 3. Summary of Magnetic Results Measured and Calculated for the Ternary Materials

sample	Θ_p(exp) (K)	Θ_p(calc) (K)	T_N(exp) (K)	T_N(calc) (K)
a-$GdP_{0.72(2)}As_{0.82(2)}$	−3(2)	0(1)	16.5(5)	16.8(5)
ht-$GdP_{0.76(2)}As_{0.24(2)}$	−1(2)	0(1)	16.5(5)	16.7(5)
a-$GdP_{0.49(2)}As_{0.51(2)}$	−4(2)	−3(1)	17.0(5)	17.6(5)
ht-$GdP_{0.51(2)}As_{0.49(2)}$	−4(2)	−3(1)	17.5(5)	17.7(5)
a-$GdP_{0.23(2)}As_{0.77(2)}$	−7(2)	−7(1)	18.0(5)	18.7(5)
ht-$GdP_{0.30(2)}As_{0.70(2)}$	−7(2)	−6(1)	18.0(5)	18.4(5)

Discussion

Solid-state precursor reactions provide an effective synthetic route to group 3–15 compounds. The gadolinium pnictides have been prepared by three methods: (1) rapid solid-state precursor ignition reactions, (2) annealing the precursor ignition products, and (3) reaction between the elements at high temperatures. In this discussion, the metathesis route will be evaluated by comparing the GdP products made by the various reaction methods, and a metathetical reaction pathway will be proposed.

Evaluation of the Metathesis Route. The various GdP products have virtually identical lattice parameters and Néel temperatures, suggesting that the three materials have equivalent compositions with high phosphorus contents. The similarity of the XRD patterns (Figure 1) and lattice parameters (Table 1) is significant because values of a_o for GdP can vary widely with composition. One group determined that the lattice parameter of large GdP single crystals varied depending on the phosphorus content, with values ranging from 5.71 Å ($GdP_{0.934}$) to 5.74 Å ($GdP_{1.00}$).[20] Deviations from 1:1 stoichiometry is common in rare-earth phosphides, but the fact that the lattice parameters found for the present materials are at the upper end of the size range (5.728 Å) suggests that these compounds have relatively high phosphorus contents, regardless of the synthetic method. Like the lattice parameter, the Néel temperature in GdP is also composition dependent, and all three samples display T_N = 16 K, corresponding to the high end of the range of reported Néel temperatures.[5,20] This result supports the idea that the phosphorus content is high in these compounds, because the Néel temperature has been shown to increase with increasing phosphorus content in the same way that the cell constants increase with increasing phosphorus content.[20]

Since the three GdP samples were shown to be single phase by XRD and EDS and have identical lattice parameters, a more sensitive characterization technique was employed to carefully differentiate between these materials. While T_N is the same for all three GdP samples, the values of Θ_p and μ_{eff} are not, because they depend critically on the paramagnetic region of the $1/\chi$ versus T data ($T > 2T_N$). Though undetectable by X-ray and EDX, the ferromagnetic impurity has profound effects on the paramagnetic results, and while i-GdP and a-GdP have similar a_o and T_N values, the small amount of free Gd metal present in i-GdP (0.04%) can be seen in the susceptibility data (Figure 4) and quantified by H-O analysis (Figure 5). This trace amount of metal disappears on further annealing, resulting in a material magnetically equivalent to that prepared from the elements at high temperatures.

The effect of annealing also can be seen in the XRD results. A 12-h anneal of the ignition products (i-GdP) leads to a more

crystalline (a-GdP) material free of metallic gadolinium. Quantitatively, the XRD line widths given by a-GdP and ht-GdP are similar, indicating that the ignition reaction coupled with a brief anneal leads to a material comparable to that produced from the elements under more extreme conditions. The effect of post-ignition heating is even more apparent in the GdSb system, as the largely amorphous i-GdSb material anneals into the rock salt structure with the same lattice parameter as the ht-GdSb sample (Figure 2).

Possible Reaction Pathways. These ignition reactions are initiated at room temperature and are essentially instantaneous, yet they often produce high-quality crystalline materials. It has been shown that the direct ignition products are XRD- and EDX-pure, and that a twelve hour anneal of the ignited precursor materials produces compounds that are at least as homogeneous, stoichiometric, and crystalline as those prepared from the elements at 1000 °C for 100 h. The effectiveness of the ignition process is due to the reaction dynamics. Aspects of the reaction process to be discussed here include initiation, thermodynamics, and a proposed mechanistic pathway.

The 3−15 reactions are initiated by local heating with a hot filament. In other ignited SSM reactions, the self-sustaining processes are initiated when one or both of the precursors melt and/or vaporize.[12−15] For the group 13−15 precursor reactions, shown in eq 8 (where M is either Al, Ga, or In; and Pn is either

$$MI_3 + Na_3Pn \xrightarrow{\text{ignite}} MPn + 3NaI \qquad (8)$$

P, As, or Sb), the self-sustaining process is thought to be initiated by melting of the MI_3 (mp < 300 °C) precursor. In the present case, it is likely that the decomposition or melting of the pnictide precursor (mp < ~850 °C) initiates the self-sustaining reactions because the melting point of GdI_3 (mp = 926 °C) is greater than the temperature reached by the hot filament (*ca.* 850 °C).

The ignited solid-state precursor reactions are rapid and very exothermic. The formation of the NaI byproduct drives this process thermodynamically. The calculated enthalpy of reaction for the synthesis of GdAs is - 89.8 kcal/mol, with the production of NaI accounting for 73% of the heat of product formation. Once the self-sustaining reactions are initiated, they generate a great deal of heat. Optical pyrometry reveals that reactions surpass 800 °C within seconds of initiation. These temperatures are sufficient to melt the byproduct salt ($mp_{(NaI)}$ = 660 °C) and/or decompose the pnictide precursors. A molten reaction flux allows for increased diffusion of the reactants, thereby overcoming solid-solid reaction barriers and permitting continuation of the self-sustaining process. Though very exothermic and quite rapid, these reactions quickly cool to room temperature in <10 s.

While the initiation processes appear straightforward, discerning the intermediate steps is quite challenging. Once initiated, the rapid, exothermic nature of these precursor reactions makes it very difficult to directly observe intermediate species or mechanistic steps by traditional solid-state techniques (e.g., XRD). Because of this difficulty, speculation about mechanisms requires one to study the end products, and then to infer the steps which might lead to these products. One can imagine that just after ignition of the reaction, under the extreme conditions produced, there may be a variety of species present, such as the byproduct NaI, precursor molecular fragments, ions in various oxidation states, and free elements.

Though the actual reaction pathway is probably quite complicated, one might model the mechanism as a competition between two different processes. The two competing models are "elemental" and "ionic" routes. In the elemental route, a redox reaction takes place between the group 3 and group 15 elements in the presence of the NaI byproduct, and the subsequent group 3−15 product forms within the molten NaI flux as a result of the overall heat of reaction. The ionic route involves reaction between the Gd^{3+} and the Pn^{3-} ions in the molten NaI flux, where thermal energy allows atomic rearrangement through attractive forces. A schematic of the competing pathways is:

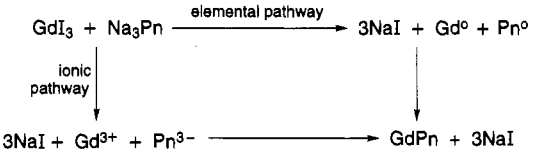

While neither of these two simplistic models can be observed directly, each does have implications which may lead to different observable reaction end products. In the elemental model, the production of group 3−15 material will take place only as long as heat is present, therefore, cooling will cause the reaction process to be quenched. This process will be limited by the amount of heat present, the ease of product formation, and the rate of cooling. In the ionic model, the effect of rapid cooling can be expected to prevent self-annealing of the products, leading to amorphous materials. The relatively short distances between the reactive ions is traversed easily at the high reaction temperatures. There are several results of particular interest which give crucial insight into which model may predominate in these systems: The ignition products contain virtually no free elements, the largely amorphous i-GdSb displays bulk magnetic susceptibility qualitatively similar to it's *crystalline* phosphide and arsenide counterparts, and the i-Gd(P, As) products have the same P:As ratios as the precursors from which they are made.

The absence of free elements in the i-GdPn systems (~10^{-2} %), can be contrasted with the group 13−15 compounds produced by analogous metathesis reactions. In this case (shown in eq 8), both metal and pnictogen are detected in the final products (>1%).[15] When GaI_3 and Na_3P are ignited together, red phosphorus is visible by optical microscopy, and gallium is seen as metallic spheres by SEM. In the InPn reactions, indium and arsenic (or antimony) are seen in XRD patterns, and phosphorus can be seen by optical microscopy. Based on the group 13−15 results, the presence of a substantial amount of elements in the end products of the group 3−15 reactions would be expected if the 'elemental' pathway were followed in the 3−15 systems, since reactions between gadolinium and phosphorus typically require long periods of time (>50 h) at elevated temperatures (>900 °C) to go to completion. Therefore, the virtual lack of free elements in the products is taken as evidence for the ionic mechanism. For the reaction to proceed via the ionic route, the cation must be stable with respect to reduction by the anion. Although the specific electrochemical studies are not known, redox potentials for Gd^{3+} and Ga^{3+} in a 450 °C KCl-LiCl melt have been reported and show that Gd^{3+} ($E°$ = −2.788 V vs Pt) is considerably more stable with respect to reduction than Ga^{3+} ($E°$ = −1.136 V vs Pt).[26]

More evidence for an ionic pathway can also be inferred from the GdSb reactions. The inverse susceptibility versus temperature curve from the amorphous i-GdSb sample is qualitatively very similar to the curves resulting from the i-GdP and i-GdAs samples, even though, the i-GdSb product is virtually amorphous

(26) Plambeck, J. A. *Encyclopedia of Electrochemistry of the Elements*; Bard, A. J., Ed.; Marcel Dekker, Inc.: New York, 1976, Vol. 10.

to X-rays. The high-temperature ($T > 3T_N$) bulk magnetic susceptibility looks like that expected for a paramagnetic substance contaminated with traces of a ferromagnetic impurity. This implies that there are Gd^{3+} ions, and that they are coordinated to antimony ions (as in the crystalline analogs), but these coordinated species have not crystallized. In this case, the reaction cools before the local Gd_xSb_y clusters can be annealed into long-range order. Crystalline order is not a prerequisite for the observed paramagnetic susceptibility, since these characteristics arise from localized Gd^{3+} ions. However, the lack of long-range structural order can explain why the Néel point is not clearly observable in the susceptibility data. It is also important that even though i-GdSb does not crystallize as well as the i-GdP and i-GdAs samples, the amorphous products do not contain any more free Gd metal. Since it is expected that the species quenched in the amorphous state would reflect the reaction intermediates, the absence of substantial amounts of free gadolinium in the amorphous powders is further evidence that the intermediates are not elemental.

Ignition reactions between GdI_3 and the solid-solution precursors $Na_3P_xAs_{1-x}$ produced the ternary compounds GdP_xAs_{1-x} with the same P and As composition as seen in the reactants, within experimental error. In this case, the stoichiometry of the ternary precursor is conserved in the product, providing further evidence for the ionic route. This can be contrasted to the analogous Ga(P, As) system where the stoichiometry of the solid-solution precursor is not conserved.[14a,15d,e] Reactions between GaI_3 and $Na_3P_xAs_{1-x}$ lead to products which enrich in phosphorus relative to the precursor composition over a range of values of x, from $x = 0.25$ to $x = 0.75$. We have suggested that those reactions proceeded through elemental intermediates, and that the selective enrichment of phosphorus was due to the fact that phosphorus has a higher vapor pressure than arsenic at the reaction temperature.[14a,15d,e] Selective enrichment of the element with the higher vapor pressure also was observed in ignited SSM reactions between $MoCl_5$ (and WCl_6) and the ternary precursors $Na_2(S, Se)$.[13c] In these reactions, the products were enriched in S relative to the precursor composition. If the present Gd(P, As) reactions were to go through elemental intermediates, then phosphorus would most likely selectively enrich compared to arsenic for the same reason phosphorus enriches relative to arsenic in the Ga(P, As) system and for the same reason that sulfur enriches relative to selenium in the Mo-$(S, Se)_2$ system. Drawing conclusions about what reaction mechanism may be active in the GdPn system based on comparisons to the Ga(P, As) and the $Mo(S, Se)_2$ systems assumes that the effect of the alkali halide flux (NaI with Gd(P, As) and Ga(P, As), and NaCl with $Mo(S,Se)_2$) is constant from one system to the next. While this assumption may not prove to be entirely valid, it does seem appropriate for a first-order approximation. Investigations into both thermodynamics and kinetics of the rapid SSM reactions are underway.

Conclusions

Self-sustaining, solid-state metathesis (SSM) reactions are effective synthetic routes to the antiferromagnetic gadolinium phosphides, arsenides, antimonides, and phosphide-arsenide solid solutions. The products of the brief (<3 s) ignited SSM reactions are single phase, XRD-pure materials free of sodium and iodine contamination, as measured by EDX. There are slight traces of free Gd metal present ($10^{-1}-10^{-2}$%, detectable only by magnetic analysis), but following a brief heat treatment (1000 °C for 12 h), the annealed ignition products are magnetically, as well as structurally, identical to the compounds prepared from the elements in the traditional, high-temperature method (1000 °C for 100 h). Solid-solution Gd(P, As) compounds have been prepared from $Na_3(P, As)$ precursors, and the P:As stoichiometries present in the precursors are conserved in the products. It is suggested that the reactions proceed through a largely "ionic" route, where upon initiation of the self-sustaining reaction, the Gd^{3+} and Pn^{3-} ions combine (under electrostatic forces) in a molten NaI flux, until the salt cools and the reaction stops.

Acknowledgment. The authors gratefully acknowledge Dr. E. G. Gillan, Dr. P. R. Bonneau and Prof. J. B. Wiley for fruitful discussions of this work. We thank Prof. C. Reed, of the Department of Chemistry at the University of Southern California, for access to the SQUID magnetometer, and Dr. R. Orosz for his help with the instrument and for useful discussions of the magnetic data. This work was supported by the National Science Foundation Grant DMR-9315914 and the Packard, Dreyfus, and Sloan Foundations (R.B.K.).